Tenth International Conference on Computational Fluid Dynamics (ICCFD10), Barcelona, Spain, July 9-13, 2018

ICCFD10-094

Nonlinearly-corrected Large Eddy Simulation for accurately evaluating both thermal efficiency and pollutant emissions in various types of engines and reactors

R. Konagaya* and K. Naitoh*
Corresponding author: rm.kngy@toki.waseda.jp
* Waseda University, Japan

Abstract: We here propose a new nonlinear numerical method of global correction for accurately evaluating fluid-dynamic instability, thermal efficiency, and pollutant emissions in large eddy simulation and direct numerical simulation of subsonic and supersonic flows of power systems including combustion engines. Emphasis is also placed on the fact that, even though a very small amount, unrealistic non-zero density of fuel obtained by traditional computational methods with the linear correction or without any correction results in numerical errors of pollutant emissions such as hydrocarbon (HC) at order of ppm. Then, this new nonlinear method of correction also targets precise evaluation of thermal efficiency proportional to total amount of CO2 exhausted.

Keywords: Numerical method, Global correction, Nonlinear, Computational Fluid Dynamics, Turbulence, Jet, Gas fuel, Engine.

1 Introduction: Problem underlying traditional computational fluid dynamics and our previous linear correction method

Improvement of thermal efficiency is expected for various power systems including combustion engines for ground and aerospace, because recent increase of carbon dioxide in atmospheric air is a big environmental problem, and because mobility systems having only electric battery, which are still very expensive, also have various problems including durability. Therefore, thermodynamic quantities in power systems must be evaluated accurately by multi-dimensional computer simulations.

Numerical errors of a few percent regarding thermal efficiency as spatially-integral value, which often happens in computational fluid mechanics especially for complex geometries such as those of power systems, are comparable to the target values set for improvement of energy systems. Thus, this is a problem for applications and engineering. The reason why traditional computational fluid mechanics cannot accurately evaluate thermodynamic quantities including thermal efficiency is related to the fact that efforts are mainly devoted for accurately obtaining spatial variations of fluid-dynamic quantities, such as shockwave and turbulence, such as those in high-speed jets on power systems including engines, power plants, and fuel cells. Each type of numerical discretization method invariably generates numerical errors on spatial variations of physical quantities, which lead to numerical errors of spatially-integrated thermal efficiency as result of cumulation.

Finite element methods applied for deterministic Navier-Stokes equation will bring relatively precise evaluation of spatially-integral values such as thermal efficiency. However, there are relatively less computations on turbulence based on finite element methods. We are still in the dilemma of spatial variations such as turbulence and space-averaged quantities like thermal efficiency.

In order to overcome this problem, a previous numerical approach of correction for global mass

conservation based on a linear correction of the form like $\rho^* = \rho + \Delta\rho$, where the density correction is $\Delta\rho$ with ρ^* as the corrected ones, for single component [1,2], show a better possibility which can compute both thermodynamic quantity and fluid-dynamic quantity, for the Navier-Stokes equation at low Mach numbers in a subsonic regime. [Naitoh and Kuwahara, 1992, Naitoh and Shimiya, 2011, Shinmura and Naitoh, 2013] This linear correction is possible because, for low Mach numbers, spatial variations of the fluid dynamic pressure are relatively small in comparison with the space-averaged thermodynamic pressure.

Let us think about supersonic or transonic flows (Fig. 1a) such as a high-speed gas jet flow of multi-components injected into a constant volume chamber. Prediction failure of penetration length often occurs, because the linear correction method for densities of component often results in unrealistic non-zero density for multi-component systems, although the density of the injected actual fuel gas inside the chamber is zero during a certain period from the onset of injection. (Fig. 1b) This non-zero density in the gas-less fuel region appears because the linear correction is performed with the form of addition at each point in the analytic domain of the chamber and nozzle. Of course, traditional computational fluid dynamics without linear corrections will also lead to certain amount of unrealistic non-zero gas fuel, which is related to numerical oscillation around the contact surface between gas fuel and oxidant or around shock wave. The errors cannot be zero, even when numerical discretization having higher order of accuracy reduces the numerical oscillation. Moreover, the linear correction is unsuitable for transonic and supersonic regimes, where density, pressure, and temperature all vary in space and time, resulting in strongly nonlinear tendencies. Thus, to cut the above long story short, there are the two important problems of global corrections: in flows at high Mach numbers and with multi-components

Therefore, we here propose a new nonlinear numerical method of global correction of fuel densities at transonic and supersonic flows.

Emphasis is also placed on the fact that unrealistic non-zero density of fuel calculated with the linear correction in Fig. 1b results in numerical errors of pollutant emissions such as hydrocarbon (HC). Thus, this new nonlinear method of correction also targets precise evaluation of pollutant emissions such as HC, NOx, and soot at the level of ppm, extremely smaller than CO_2, which was difficult to achieve by previous computational fluid mechanics or by our previous linear correction [Naitoh and Kuwahara, 1992].

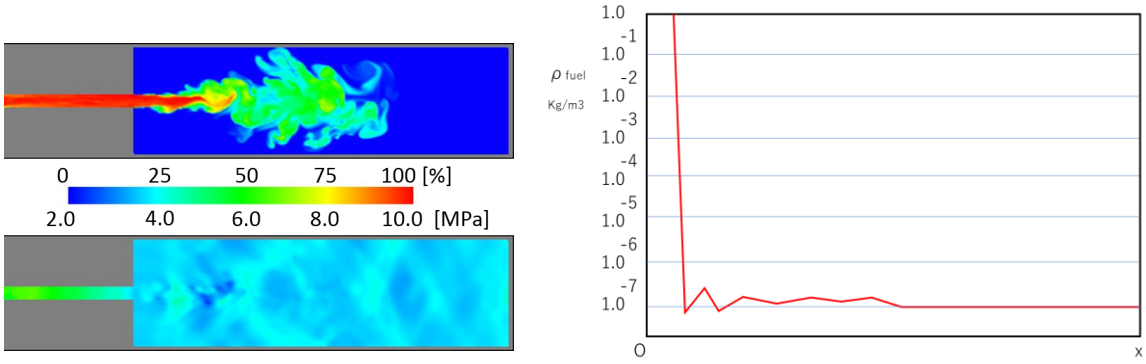

(a) (b)

Figure 1: Computation (LES) of a high-speed gas jet flow. (a) Hydrogen gas volume ratio (top) and pressure (bottom) distribution at 0.780ms, computed with tank pressure of 10MPa and chamber pressure of 3.5MPa. (b) Image of numerical errors around contact surface or shock front.

2 Governing equations and numerical methods

Here, we used the unsteady three-dimensional compressible Navier-Stokes equation for multi-components expressed in a multi-level formulation (Naitoh and Kuwahara, 1992, Naitoh and Shimiya,

2011, and Shinmura et al., 2013) for the velocity, pressure, density, and temperature in Eqs. (1)-(7) described in Section 2.1, which includes the equation of state and the RNG subgrid turbulence model with fewer arbitrary constants because they are derived theoretically without any experimental data (Yakhot and Orszag, 1986). In Section 2.2, the equation of Eq. 8 is added for evaluating accurately spatial gradients (Majda and Sethian, 1985, Naitoh and Kuwahara, 1992, Naitoh and Shimiya, 2011).

In Section 2.3, the numerical method used for discretization and the algorithm are described.

The most important point of the present paper is a new nonlinear formulation of Eqs. 9 and 10 proposed in Section 2.4 for correcting total conservativity of thermo-dynamic quantities, which enables an accurate numerical evaluation of thermal efficiency at level of percent and emissions at level of ppm for various energy systems including combustion engines at various Mach numbers.

2.1 Governing equations and correction equations

2.1.1 Governing equations concerning mixed air

Equations 1-4 as the basic equations are of momentum, energy, and mass conservation laws, and equations of state, respectively.

$$\frac{Du_i}{Dt} = -\frac{1}{\rho_{mix}} p_{mix,i} + \nu_{T_{mix}} \left(u_{i,j} + u_{j,i} - \frac{2}{3} u_{k,k} \delta_{ij} \right)_{,j} \tag{1}$$

$$\frac{DT_{mix}}{Dt} = -\frac{1}{C_{p_{mix}} - R_{mix}} \frac{p_{mix}}{\rho_{mix}} \overline{D} + \frac{1}{C_{p_{mix}} - R_{mix}} \frac{1}{\rho_{mix}} \left\{ -q_{T\,i,i} + \nu_{T_{mix}} \times \rho_{mix} \left(u_{i,j} + u_{j,i} - \frac{2}{3} u_{k,k} \delta_{ij} \right) u_{i,j} \right\} \tag{2}$$

$$\overline{D} = -\frac{C_{p_{mix}} - R_{mix}}{C_{p_{mx}}} \frac{1}{p_{mix}} \frac{Dp_{mix}}{Dt} + \frac{1}{\rho_{mix} C_{p_{mix}} T_{mix}} \left\{ -q_{T\,i,i} + \nu_{T_{mix}} \times \rho_{mix} \left(u_{i,j} + u_{j,i} - \frac{2}{3} u_{k,k} \delta_{ij} \right) u_{i,j} \right\} \tag{3}$$

$$p_{mix} = \rho_{mix} R_{mix} T_{mix} \tag{4}$$

In Eqs. 1-4, quantities of $u_i, \rho, p,$ and T denote velocity vector, density, pressure, and temperature, respectively, while subscript *mix* refers to all of the components of air and fuel in the flow field. The subscripts of the spatial derivatives with Einstein's notation and $\overline{D}$ used in the equations above are defined as the divergence of velocity. Heat flux $q_{T,i}$=-$k_T T_{,i}$ is calculated with the turbulent thermal diffusion constant k_T, while ν_T is the turbulent kinetic viscosity coefficient (Naitoh and Kuwahara, 1992, Naitoh and Shimiya, 2011, Shinmura, Kubota, and Naitoh, 2013). (In the present paper, we use the equation of state for perfect gas because the real gas effect ascribable to hydrogen gas at nearly atmospheric temperature is fairly small.)

2.1.2 Governing equations concerning fuel (conservation law of mass)

The temporal change in the spatial distribution of fuel is calculated by the law of conservation of mass in Eq. (5).

$$\frac{D\rho_{fuel}}{Dt} = -\rho_{fuel} u_{i,i} + D_T \rho_{fuel,ii} \tag{5}$$

where subscript fuel means vaporous fuel such as hydrogen injected from a nozzle and D_T denotes the turbulent diffusion coefficient.

The turbulent coefficient of kinematic viscosity is calculated with Eq. (7), which is a simplification of the Yakhot-Orszag subgrid turbulence model (Yakhot and Orszag, 1986) for LES shown in Eq. (6).

$$\nu_{T_{mix}} = \nu_0 \left[1 + H\left\{ \frac{C_S \Delta^4}{\nu_0^3} \nu_{T_{mix}} \left(u_{i,j} + u_{j,i} \right)^2 - 75 \right\} \right]^{\frac{1}{3}} \tag{6}$$

with

$$\nu_{T_{mix}} = \nu_0 \left\{ \frac{C_S \Delta^4}{\nu_0^3} \nu_{T_{mix}} \left(u_{i,j} + u_{j,i} \right)^2 \right\}^{\frac{1}{3}} \qquad C_S{}^2 = \frac{0.06}{(2\pi)^4}, \ \Delta = C_g \Delta x \tag{7}$$

Constant C_S is determined theoretically without any experimental data (Yakhot and Orszag, 1986), while C_g can have a value between 1.0 and 2.0 logically and is here set at 1.0. Turbulent thermal- and mass-diffusion coefficients are also calculated by using Eq. (7) with the Schmidt number of 0.7 (Tominaga and Stathopoulos, 2007) and Prandtl number of 0.71 (Yakhot and Orszag, 1986). (The influence of constants in the subgrid turbulence models for LES on the mass diffusion process is not large (Tominaga and Stathopoulos, 2007). Thus, we use this value for the Schmidt number, which is often used.)

2.2 Evaluation method of spatial gradients

Here, as an additional equation, we add the spatial gradient of Eq. 1, which accurately evaluates the spatial gradient of pressure related to turbulence (Mazda and Sethian, 1985, Naitoh and Kuwahara, 1992, Naitoh and Shimiya, 2011, Shinmura, Kubota, and Naitoh, 2013), i.e., Eq. 8.

$$p_{mix,ii} = -\rho_{mix} \overline{D}_{,t} - \rho_{mix} \left(u_j \, u_{i,j} \right)_{,i} + \left(\frac{\rho_{mix,i}}{\rho_{mix}} \right) p_{mix,i} + \rho_{mix} \left[\nu_{T_{mix}} \left(u_{i,j} + u_{j,i} - \frac{2}{3} u_{k,k} \delta_{ij} \right)_{,j} \right]_{,i} \tag{8}$$

It should be stressed that the partial differential equation of pressure, which eliminates the divergence of velocity from Eqs. 3 and 8, clearly shows hyperbolic (wave type) or elliptic (Poisson type) ones, according to the two terms on the right-hand side of Eq. 3, i.e., two types of density variations explicitly described for the effects of wave propagation such as sound and diffusion.

In cases having the two types of density variations related to the wave effect and heat transfer, the divergence of velocity, i.e., mass conservation law on overall density, should be evaluated by both of the two terms on the right-hand side of Eq. 3, respectively, although the two terms become zero, which is the mass conservation law for incompressible flows without density variations,

$\overline{D} \equiv u_{i,i} = \dfrac{\partial u_i}{\partial x_i} = 0$.

In cases of low Mach numbers, the first term on the right-hand side of Eq. 3 can be eliminated approximately, resulting in less computational time. This is because the time increment determined by the Courant number can have a larger value for an incompressible flow, if the coupling effect between sound waves and turbulence generation is not important.

2.3 Numerical algorithm for spatial variations

In order to solve Eqs. 1-8, we use a computational method identical to that of C-CUP (Yabe and Wang, 1991, Takewaki et al., 1985). This algorithm, which mathematically matches well the governing equation systems in Eqs. 1-8 shown above, makes it possible to uniformly handle both compressible and incompressible flows in the same calculation domain.

Generally, flow fields are constructed by the coexistence or balance of advection, acoustic, and diffusion phases. This algorithm handles these three phases by separating them according to their characteristic velocity. The calculation is done by adding the effect of each phase. First, we calculate the advection phase with strong nonlinear convection in Eqs. (1)-(3) and (5). The equation having only the convection terms for the advection phase is calculated with the CIP method with a higher order of accuracy (Yabe and Wang, 1991, Takewaki et al., 1985), which uses a cubic interpolation function with less numerical diffusion. Here, the wave-Poisson equation of pressure in Eqs. (3) and (8), obtained by taking the spatial derivation of Eq. (1), is also computed as a correction (Yabe and Wang, 1991, Takewaki et al., 1985), which can be done by an inverse matrix calculation such as the

successive over-relaxation (SOR) method (Roache, 1976). An interpolation check is also added during this calculation to control nonphysical oscillation and to maintain monotonicity (Himeno et al., 2010). Next, we calculate the non-advection phases, which include only the acoustic and diffusion phases (Yabe and Wang, 1991, Takewaki et al., 1985).

2.4 Global correction method of nonlinear type for spatial average values in multi-component system

For power source systems such as engines or closed reactors, thermodynamic quantities must be evaluated accurately by computer simulations because numerical errors of a few percent concerning performance such as efficiency are often comparable to the target values set for improvement of energy systems and also because emissions such as hydrocarbon (HC), soot, and NOx are of the order of ppm, much less than percent.

Here, we propose and use a new nonlinear numerical method of correction efficient even for transonic and supersonic flows such as gas jet flows injected from nozzle to chamber in Fig. 2.

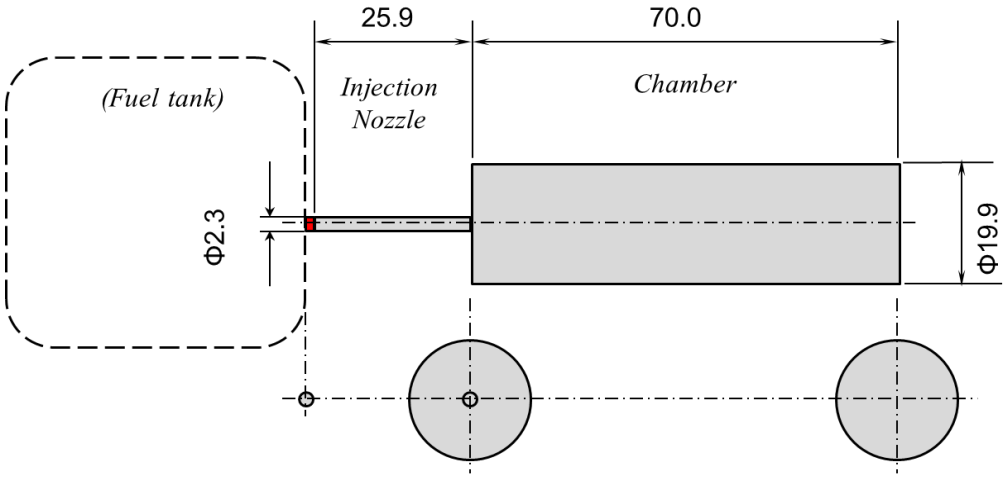

Fig. 2 Subject domain of computations. The valve installed in the nozzle is shown in red.

Equations 9 and 10 bring accurate nonlinear corrections according to the mass conservation laws for the mixture and fuel, respectively

$$\rho^{*}_{mix}(t,x_i)=\rho_{mix}(t,x_i)\times\frac{\int_{Vall}\rho_{mix}(t=0,x_i)\,dV+\int_{t>0}\dot{m}\,dt}{\int_{Vall}\rho_{mix}(t,x_i)\,dV} \tag{9}$$

$$\rho^{*}_{fuel}(t,x_i)=\rho_{fuel}(t,x_i)\times\frac{\int_{t>0}\dot{m}\,dt}{\int_{Vall}\rho_{fuel}(t,x_i)\,dV} \tag{10}$$

where the superscript * indicates values after correction and $\dot{m}$ denotes the fuel mass injected per time from an inlet boundary such as the valve in the injection nozzle shown in Fig. 2.

For both the densities of the mixture and fuel shown in Eqs. 9 and 10, corrections are done by multiplying the correction term of

$$\frac{\int_{Vall} \rho\ (t=0,\ x_i)\ dV + \int_{t>0} \dot{m}\, dt}{\int_{Vall} \rho(t,\ x_i)\, dV} \tag{11}$$

between 0 and 1.0 to tentative densities.
When total masses in chamber of

$$\int_{Vall} \rho(t,\ x_i)\, dV$$

have numerical errors, densities are corrected by

$$\int_{t>0} \dot{m}\, dt\ .$$

It is emphasized that the nonlinear calculation method, i.e., multiplication of the nonlinear correction terms in Eqs. 9 and 10, essentially differs from that in a previous approach for mass conservation, which is based on a linear correction of the form of $\rho^* = \rho + \Delta\rho$, where $\Delta\rho$ denotes the additional term for subsonic regions shown in Eqs. 12 and 13 (Naitoh and Kuwahara, 1992, Naitoh and Shimiya, 2011).

$$\rho^*_{mix}(t, x_{\rho fuel>0}) = \rho_{mix}(t, x_{\rho fuel>0}) + C_{cx} \times \frac{\left(\int_{Vall} \rho_{mix}(t=0,\ x_i)\ dV + \int_{t>0} \dot{m}\, dt\right) - \int_{Vall} \rho_{mix}(t,\ x_i)\, dV}{\int_{Vall} dV} \tag{12}$$

$$\rho^*_{fuel}(t, x_{\rho fuel>0}) = \rho_{fuel}(t, x_{\rho fuel>0}) + C_{cx} \times \frac{\int_{t>0} \dot{m}\, dt - \int_{Vall} \rho_{fuel}(t,\ x_i)\, dV}{\int_{V_{\rho fuel>0}} dV} \tag{13}$$

where C_{ex} denotes an arbitrary constant between 0.0 and 1.0.

Emphasis is placed on the fact that, for multi-component systems, this correction method of linear addition shown in Eq. 13 often results in unrealistic non-zero density in the chamber far from the injection point, although the actual density of the fuel gas injected from nozzle is zero in the chamber during a certain period from the onset of injection. This non-zero density in the region without fuel appears because the linear correction based on Eq. 13 is performed with the form of addition at each point in the analytic domain of the chamber and nozzle, i.e., as base-up, whereas the nonlinear correction due to Eq. 10 results in zero fuel at the points without fuel because multiplication of zero by no fuel is zero.

Equation 10 is important, because usage of Eq. 13 or without linear corrections often lead to non-zero density in no fuel region due to numerical oscillations around contact surface between gas fuel and oxygen, even though numerical schemes with higher-order of accuracy such as the CIP methods (Yabe and Wang, 1991, Takewaki et al., 1985), TVD methods (LeVeque, 1992), or compact schemes are employed for convection terms.

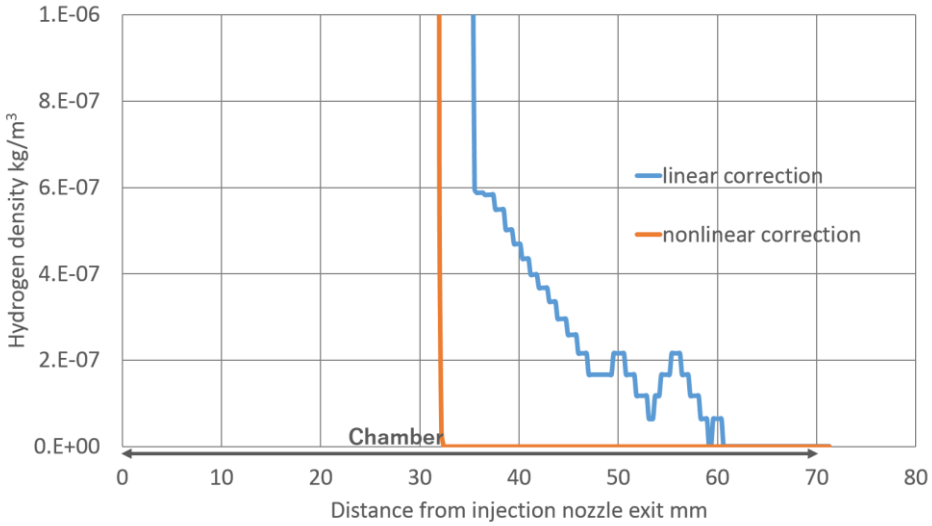

Fig. 3 Comparison of hydrogen density along the jet axis for linear and nonlinear correction methods at 0.423ms

Figure 3 shows the computational results obtained with the previous linear correction method described in Eq. 13 (or without any correction) and the new nonlinear correction method denoted in Eq. 10, for the hydrogen density along the jet axis at the center of the chamber in Fig. 2. The previous linear correction method with Eq. 13 often miscalculates the penetration length of gas jets with unrealistic gas fuel ratio of the order of ppm, implying a gas jet closing to the wall at the right edge in Fig. 2, when actually the jet has only entered the chamber. This problem shown in Fig. 3 comes from a very small amount of gas fuel caused by numerical error related to numerical instability around discontinuous physical quantities. On the other hand, the nonlinear shape of Eq. 10 maintains the fuel density to be zero at grid points where injected gas does not exist.

Even a small amount of false non-zero density will bring unrealistic unburned fuel at level of ppm, i.e., emissions such as hydrocarbons (HC). Other emissions such as NOx, and soot, which are also at ppm level, should be calculated accurately, because zero-emission vehicle (ZEV) is today demanded for automobiles, which is evolved from low emission vehicle (LEV). Thus, the nonlinear correction method based on Eq. 10 is very important.

This nonlinear correction method based on Eqs. 9 and 10 is also very important and necessary for evaluating performance such as the thermal efficiency of engines and power systems. This is because numerical errors invariably occur for density, pressure, and temperature in numerical simulations, even if the finite volume method is used with detailed chemical reaction models in very high accuracy. These numerical errors, which originate around the contact surface between gas fuel and oxidant and also from large temperature gradients around chamber walls, will often make trials of performance improvement impossible because improvement of the thermal efficiencies and emissions of engines and energy systems today is often done at very small rates of 1-3%. The present numerical method compensates numerical error on the total mass is zero. This is a basic and important aspect for various CFD models. For general-purpose numerical codes including OpenFoam, this problem of false density will be especially serious, because it is used by many people.

Moreover, there is another important point in the global correction. For incompressible and subsonic flows even in cases with combustion such as premixed flame and diffusion flame, spatial variations of the fluid dynamic pressure gradient are relatively small in comparison with the space-averaged thermodynamic pressure. Then, the equation of state (with the form of $p = \rho \times R \times T$ or the modified versions for supercritical state) results in a linear relation between pressure and temperature for incompressible flows having constant density. Thus, Eq. 12 for mixture density, temperature, and pressure with the linear form of addition at each point in the analytic domain of the chamber and nozzle are allowable for incompressible and subsonic regimes. (Equation 12 is effective only for low

Mach number conditions because C_{ex} = 1.0 leads to constant density in space.) On the other hand, for transonic and supersonic regimes, density, pressure, and temperature all vary in space and time, resulting in strongly nonlinear tendencies. Thus, we found that the nonlinear form of Eqs. 9 and 10 may be much better for transonic and supersonic regimes.

Thus, in the present study, the multi-level formulation with Eqs. 1-8, which is extended by adding of Eqs. 9 and 10, is employed.

More concretely, even finite volume methods based on the conservative form of the governing equations produce numerical errors for the conservation of physical quantities. Thus, the present correction method is useful for several types of computational fluid dynamics problems, especially for power systems including engines.

3 Details of subject domain with nozzle for injecting gas jet and mixing chamber and computation conditions

3.1 Nozzle for injecting gas jet and mixing chamber

The subject domain of this research where computations are done is the mixing closed chamber and nozzle shown in Fig. 2. The closed chamber has a constant volume, and there is a disc wall on each of its right- and left- hand sides. The chamber in Fig. 2 has an axisymmetric geometry for making a comparison with experimental penetration data of gas jets injected into an open area (Hamamoto et al., 1987, Tsujimura et al., 2006). Then, we also defined the chamber volume in Fig. 2 to be of the order of actual engines, and the diameter ratio of the chamber and nozzle is also of the order of that of actual engines. The gas fuel tank is located on the left-hand side of the nozzle in Fig. 2, although not included in the actual calculation region.

In the present report, a valve is installed at the inlet of the nozzle (at outlet of the gas fuel tank), which opens suddenly like diaphragm in shock tube at 0.2 millisecond and also closes suddenly at 2.1 millisecond.

3.2 Computation conditions

Computations of single-component hydrogen jets were done under initial conditions of a fuel tank pressure of gaseous fuel = 10 MPa and back pressure (chamber pressure) of air = 3.5 MPa, i.e., the pressure level inside the combustion chamber after piston compression in the engine (Takagi et al., 2016). The initial temperature was 293.15 K and the initial velocities were zero in the combustion chamber including the nozzle.

The fuel tank pressure and temperature were fixed at 10 MPa and 293.15 K during the mixing process and were given at the inlet boundary of the nozzle. The velocity in the fuel tank was zero. The non-slip condition of velocity was given for the walls of the nozzle and combustion chamber, including the disc wall located on the right-hand side, while the Neumann condition (dp/dn=0, where n is the unit vector normal to the wall) was given for pressure on the walls. The temperature on the walls of the combustion chamber including the nozzle was given under an adiabatic condition.

The flow within the chamber and nozzle was calculated with 5,100,000 (472×104×104) grid points, and a grid size of $\Delta x=\Delta y=\Delta z$=0.209 mm, while the Courant number was set to be 0.1. [The mean value of the Reynolds number at the exit of the injection nozzle while fuel was injected was about 8.6×10^5 for the hydrogen jet. The value of the Reynolds number at the middle of the chamber (35 mm from the nozzle exit) was about 2.2×10^4 for the hydrogen jet. The present grid size is a little larger than the Kolmogorov scale of about 0.1 mm for evaluating turbulent mixing regions having vortices (Pope, 1987), which are relatively far from the injection point. The grid size is much smaller than the 0.5 mm size employed for simulating cyclic variations of turbulent combustion under stratified charge conditions in a direct-injection gasoline engine (Shinmura et al., 2013).]

4 Computational result of gas jet having turbulent flow and shock front

Figures 4, 5, and 6 demonstrate time-dependent distributions in space for density, pressure, and temperature, respectively. Wrinkle of contact surface between gas fuel and air generated by turbulence is computed in Fig. 4, while a very weak shock wave in Fig. 5 and low temperature region expanded after high speed flow in Fig. 6, which agree fairly well with theoretical evaluations, are observed.

For penetration length plotted against time after injection start, the computation result agrees fairly well with experimental data shown by Hamamoto et al., although some discrepancy is observed, which will be related to the difference on valve opening process.

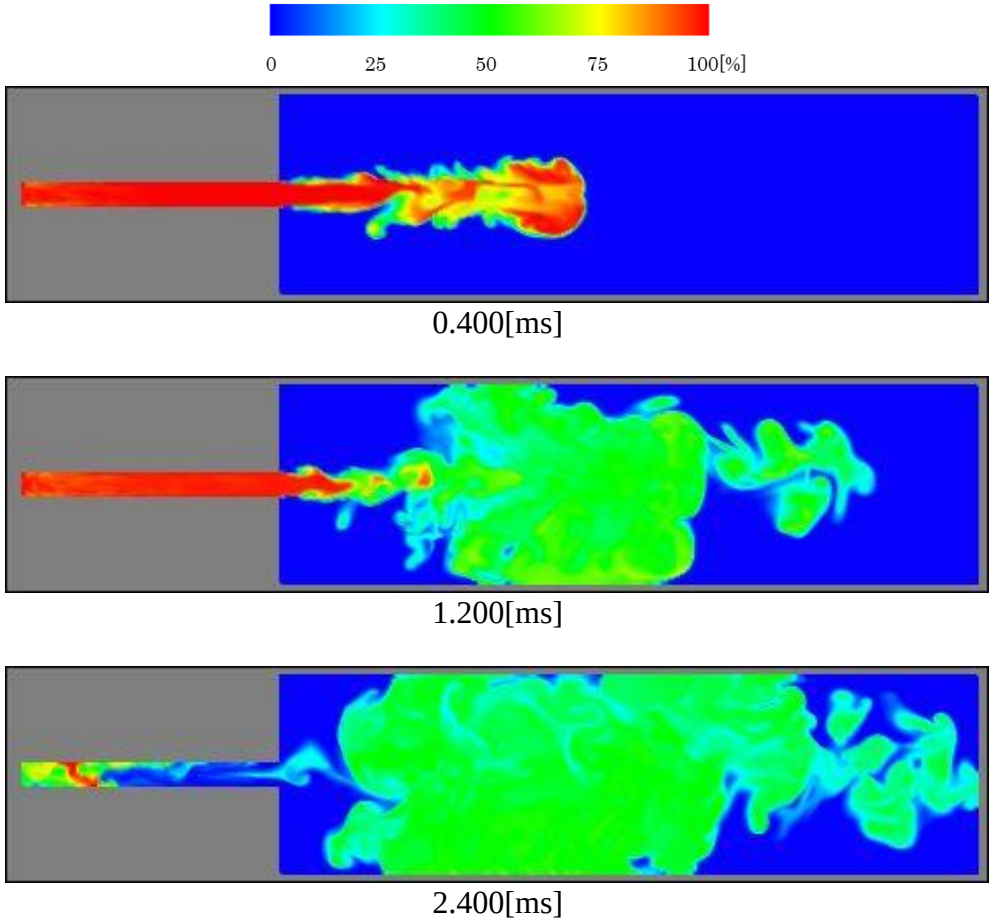

Fig. 4 Time-dependent distributions in space for volume ratio of gas fuel density

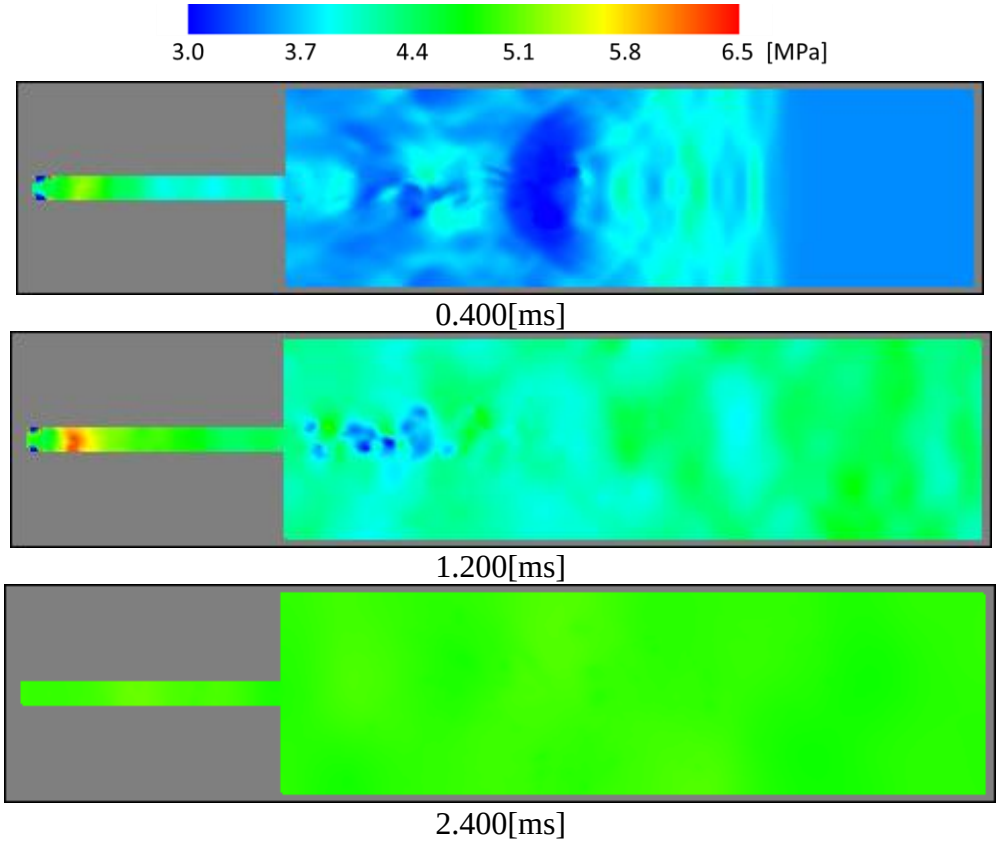

Fig. 5 Time-dependent distributions in space for pressure

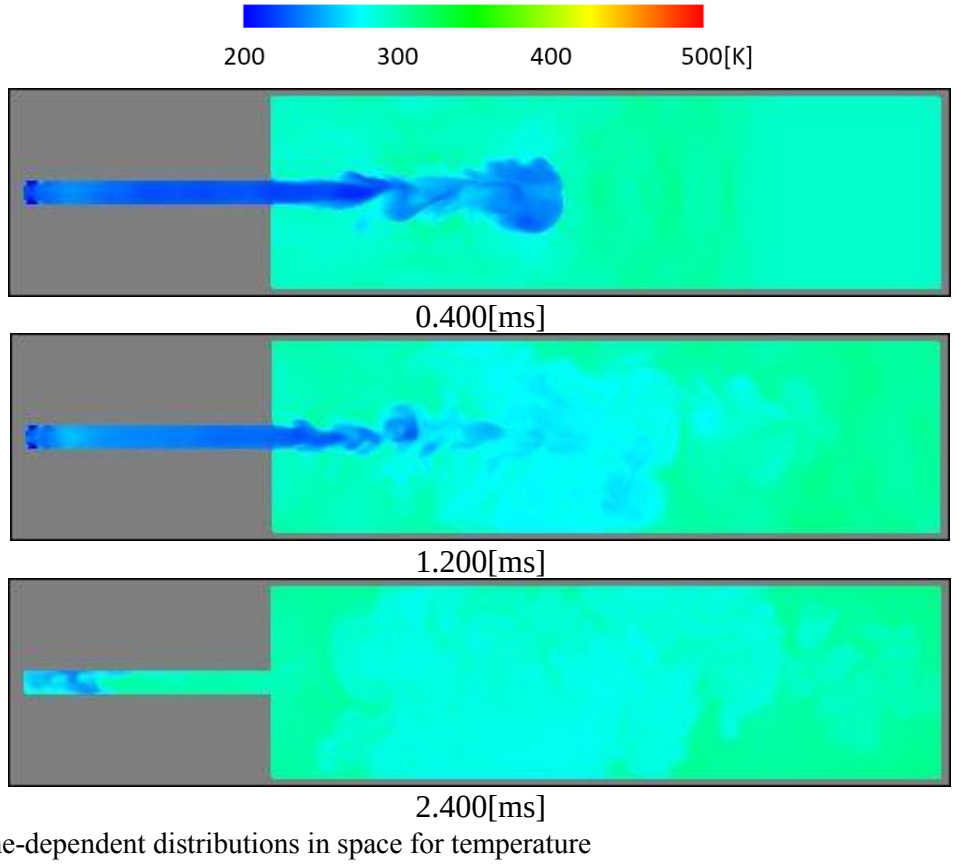

Fig. 6 Time-dependent distributions in space for temperature

5 Potential evaluating both combustion stability and emissions

The above computations based on governing equations of the unsteady three-dimensional compressible Navier-Stokes equation for multi-components expressed in a multi-level formulation [1,2] for the velocity, pressure, density, and temperature, the equation of state, and the RNG subgrid turbulence model [3], which were done at a very lean fuel condition showed a low emission and stable combustion of hydrogen at delayed ignition in a piston engine, which correspond to the data in actual combustion experiments [5], by considering the well-known tendency [4].

6 Conclusion

People think that increase of combustion engines for automobiles and motorcycles is expected to continue, because of the new big market including Africa much larger than America, while hybrid systems having combustion engines may increase. Then, improvement of thermal efficiency for engines of aircrafts and rockets increasing is also an important target.

The proposed nonlinear correction method based on Eqs. 1 and 2 is simple but very important and necessary for evaluating performance such as thermal efficiency and emissions of power source systems at various Mach number from subsonic to supersonic regimes, whereas computations based on discretizations such as traditional finite difference, finite volume, and finite element approaches will often generate spatial fluctuations of gaseous fuel related to numerical errors, which may originate from large temperature gradients around chamber walls or contact surfaces between species.

Acknowledgments

This work was supported by Grant-in-Aid for JSPS Fellows (18J22401). Also, this work was partly achieved through the use of large-scale computer systems at the Cybermedia Center, Osaka University.

References

[1] Naitoh, K., and Kuwahara K., Large eddy simulation and direct simulation of compressible turbulence and combusting flows in engines based on the BI-SCALES method, Fluid Dynamics Research 10 (1992), pp. 299-325.
[2] Naitoh, K., and Shimiya, H., Stochastic determinism for capturing the transition point from laminar flow to turbulence, Japan J. of Industrial and Applied Mathematics 28 (2011), pp. 3-14.
[3] Yakhot, V., and Orszag, S.A., Renormalized group analysis of turbulence I. Basic theory, J. Sci. Computing 1 (1986), pp. 3-51.
[4] Murayama, T. and Tsunemoto, H., Engineering of automobile engine. TDU press. (2009).
[5] Takagi, Y., Mori H. et al., Optimization of Fuel Jet Geometry, Injection Timing and Ignition Timing Focusing on Improving Thermal Efficiency in Direct Injection Hydrogen Engines, J. of JSAE 47, No. 3 (2016